Int. J. Heat Mass Transfer. Vol. 21, pp. 875–884

0017-9310/78/0701-0875 $02.00/0

FILM CONDENSATION OF BINARY MIXTURE FLOW IN A VERTICAL CHANNEL

S. KOTAKE*
Institut fur Strömungslehre der Technischen Universitat Wien, Austria

(*Received* 13 *July* 1977)

Abstract—Film condensation of binary-mixture laminar flows in a vertical channel of variable circular cross-section is studied by employing the integral method for the vapor flow and the Nusselt model for the liquid film flow. Effects of the channel geometry, vapor flow speed, vapor flow direction and the type of binary mixture on condensation behavior are predicted. The behavior is affected appreciably by the liquid–vapor equilibrium characteristics and the mass transfer process in the vapor flow. Nozzle-type flows yield larger values of local condensation rate, although the channel geometry has not a considerable effect on the overall condensation rate. The flow direction has an appreciable influence on the condensation rate and film thickness.

NOMENCLATURE

C, mass fraction of volatile component;
c_p, specific heat at constant pressure;
D, binary diffusion coefficient;
Gr, Grashof number, $\rho_r^2 g R_0^3/\mu_r^2$;
g, acceleration of gravity;
He, Stefan number, $\bar{c}_{pr}(T_{00}-T_w)/\lambda_r$;
k, thermal conductivity;
L, length of cooled wall;
Mc, Mach number, $(\rho_r U_{00}^2/P_0)^{1/2}$;
$\dot{m}$, condensation rate of mixture per unit interface area;
$\dot{m}_c$, condensation rate of volatile component per unit area;
Pr, Prandtl number, $\mu_r c_{pr}/k_r$;
P_0, vapor-flow inlet pressure;
p, pressure;
q, heat flux per unit wall surface area;
R, radius of channel;
R_0, radius of channel at vapor-flow inlet;
R_c, radius of concentration layer;
R_t, radius of temperature layer;
Re, Reynolds number, $\rho_r U_{00} R_0/\mu_r$;
R_δ, radius of vapor-flow passage, $R-\delta$;
r, radial coordinate;
Sc, Schmidt number, $\mu_r/(\rho_r D_r)$;
T, temperature;
T_w, cooled wall temperature;
u, axial velocity component;
v, radial velocity component;
X, mole fraction;
x, axial coordinate.

Greek symbols

γ, activity coefficient;
δ, condensate film thickness;
θ, dimensionless temperature, $(T-T_w)/(T_{00}-T_w)$;
λ, latent heat of vaporization;
μ, dynamic viscosity;
ρ, density.

Subscripts

e, equilibrium;
i, liquid–vapor interface;
0, center of channel;
00, vapor-flow inlet;
r, reference state.

Superscripts

$^-$, condensate liquid;
*, $x^* = x/(ReSc)$, $\dot{m}^* = ReSc\dot{m}$.

1. INTRODUCTION

FILM condensation of binary mixtures is one of the most important processes of chemical engineering. The number of theoretical and experimental works devoted to this problem, however, is rather limited [1–9], although from the phenomenological point of view considerable works have been done [10, 11].

Theoretical elaboration of the gravity-flow film condensation of a binary mixture on a cooled vertical plate was given by Sparrow and Marschall [2], on the basis of the conservation laws with an analytical model of boundary-layer flows of the condensate and vapors. With the application of such a method of analysis, Denny and Jusionis [3] investigated the effect of forced flow on film condensation of binary mixtures on a vertical flat plate. In these theoretical works, the conservation equations of boundary-layer flow are numerically solved for the vapor flow, whereas for the condensate film, the Nusselt assumption of negligible effects of liquid acceleration and energy convection is employed. The obtained results show that the heat flux toward the wall has a marked dependence on the bulk composition of binary mixture and the overall temperature difference of the system, having a minimum at a certain bulk composition. Experimental works concerning film condensation of binary mixtures on

*Visiting professor, 1976–77, Institute of Space and Aeronautical Science, The University of Tokyo, Tokyo, Japan.

external bodies have been reported by several investigators, mainly from the standpoint of heat-transfer problem [7, 8].

The problem of film condensation of binary mixtures in a tube is a case often encountered in practice, although relatively little work of it appears to have been done. Van Es and Heertjes [9] studied the channel-flow film condensation of binary mixtures with a simplified model of the vapor and liquid flows and obtained a qualitative agreement with their experimental results.

Most of the peculiar phenomena in the condensation of mixtures originate in the fact that the equilibrium concentration in phases will generally differ for each component. Due to the concentration difference, the liquid phase contains less of the volatile component than does the vapor. The volatile component of the vapor adjacent to the liquid must be removed away to supply the material of condensation. Thus, the mass transfer process controls directly the rate of condensation. In the case of internal flows, due to a sink of vapor at the liquid–vapor interface, the mass composition, velocity and temperature of the vapor flow are to be changed appreciably in the flow direction. This is the inherent feature of condensation in channel flows different from that of condensation on external bodies.

The present study is concerned with film condensation of binary mixture flows in a vertical channel. A binary mixture of vapors, both components of which are condensable, is introduced to flow downward (co-current flow) or upward (counter-current flow) into a circular channel of variable cross-section. The condensate is formed adjacent to the surface of the cooled wall, being a binary mixture of liquids, and flows downward along the wall under the action of gravity. The analytical model employed here consists of a thin liquid-layer flow adjacent to the wall and an inner vapor flow. Both flows are assumed to be steady and laminar, having an interfacial boundary of infinitesimally thin thickness. The conditions of transport fluxes and equilibrium state at the interface couple two flow fields to yield a set of governing equations. To solve the system of equations, the integral method and the Nusselt assumption are employed for the vapor flow and the liquid film flow, respectively. The effects of the channel geometry, the vapor flow speed and direction, the temperature difference of the system, and the type of mixture are studied on the behavior of film condensation.

2. PHYSICAL MODEL AND ANALYSIS

A saturated binary mixture of vapors is introduced downward or upward into the inlet of a vertical channel. The mixture has a fully developed velocity profile and a uniform temperature T_{00}, and the mass fraction of the volatile component C_{00}, corresponding to the saturation state at the temperature T_{00} and the inlet pressure P_0. Downward distances in the direction of gravity are measured in terms of the x-coordinate,

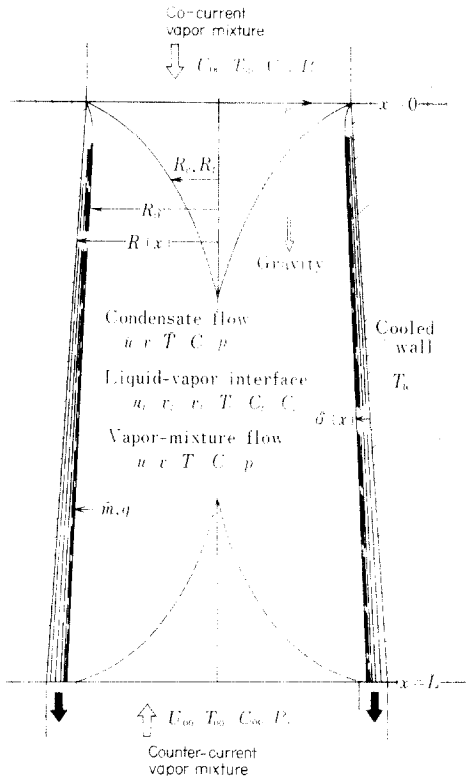

FIG. 1. Film condensation of binary mixtures in a vertical channel.

and radial distances are denoted by r. The corresponding velocity components are u and v, respectively. The flow configuration is illustrated in Fig. 1. Between the inlet and the outlet of the flow, the channel wall is cooled isothermally at a constant temperature T_w. Flowing through the channel of radius $R(x)$, the vapor mixture condenses onto the cooled wall, and changes its velocity $u(x, r)$, $v(x, r)$, temperature $T(x, r)$, and mass fraction of the volatile component $C(x, r)$. The condensate flows downward under the action of gravity force to form a thin liquid layer of thickness $\delta(x)$. The binary mixture of liquids in the film has the velocity $\bar{u}(x, r)$, $\bar{v}(x, r)$, temperature $\bar{T}(x, r)$, and mass fraction $\bar{C}(x, r)$, where the superscript (¯) refers to the liquid mixture. The condensate film flow is affected additionally by the viscous force of the vapor flow to be accelerated or decelerated depending on the flow direction. Between the condensate and the vapor, there is no relaxation layer assumed for the phase transition. The interface is of infinitesimally thin thickness, and the mixtures there are in equilibrium state corresponding to the temperature $T_i(x)$ and the pressure $p(x)$, having the mass fraction of the component vapor $C_i(x)$ and of the component liquid $\bar{C}_i(x)$.

Because of thin film thickness, the variation of flow variables is highly strong across the film compared with that in the axial direction. The diffusive transports of the vapor mixture in the flow direction are also less effective in comparison with those in the radial direction except for the very short distance close to the starting point of condensation. Thus, for both flows of the vapor mixture and the condensate, the governing

equations of boundary-layer type can be employed to account for the conservation of mass, momentum, species and energy. Although the problem involves the phase equilibrium characteristics inherent to each combination of binary components, it is useful from the fluid-dynamical standpoint to express flow variables in a dimensionless form by introducing non-dimensional parameters. In such a dimensionless form, the governing equations are written as

$$\frac{\partial}{\partial x}(\rho u)+\frac{1}{r}\frac{\partial}{\partial r}(r\rho v)=0 \tag{1}$$

$$\frac{\partial}{\partial x}(\rho uu)+\frac{1}{r}\frac{\partial}{\partial r}(r\rho vu) = -\frac{1}{M_c^2}\frac{\mathrm{d}p}{\mathrm{d}x}+\frac{G_r}{Re^2}\rho+\frac{1}{Re}\frac{1}{r}\frac{\partial}{\partial r}\left(r\mu\frac{\partial u}{\partial r}\right) \tag{2}$$

$$\frac{\partial}{\partial x}(\rho uC)+\frac{1}{r}\frac{\partial}{\partial r}(r\rho vC)=\frac{1}{ReSc}\frac{1}{r}\frac{\partial}{\partial r}\left(r\rho D\frac{\partial C}{\partial r}\right) \tag{3}$$

$$c_p\frac{\partial}{\partial x}(\rho u\theta)+c_p\frac{1}{r}\frac{\partial}{\partial r}(r\rho v\theta) = \frac{1}{RePr}\frac{1}{r}\frac{\partial}{\partial r}\left(rk\frac{\partial\theta}{\partial r}\right)+\frac{1}{ReSc}\rho c_p' D\frac{\partial C}{\partial r}\frac{\partial\theta}{\partial r} \tag{4}$$

where the second-order effects of thermal diffusion, viscous dissipation and compressible heating are neglected. The pressure can be assumed to be constant across the cross-section. The length scale, velocity and pressure are nondimensionalized by the channel radius at the flow inlet R_0, the vapor flow velocity at the inlet U_{00}, and the inlet pressure P_0, respectively. The dimensionless temperature θ is defined as

$$\theta=\frac{T-T_w}{T_{00}-T_w} \tag{5}$$

The physical properties of density ρ, dynamic viscosity μ, thermal conductivity k, specific heat at constant pressure c_p, and binary diffusion coefficient D are nondimensionalized by their own respective reference values which are denoted by subscript r. c_p' is the difference of specific heats between the binary components, $c_p'=c_{p1}-c_{p2}$. Dimensionless parameters relevant to these properties are as follows.

$$Re=\frac{\rho_r U_{00}R_0}{\mu_r}\quad Pr=\frac{\mu_r c_{pr}}{k_r}\quad Sc=\frac{\mu_r}{\rho_r D_r}$$
$$Gr=\frac{\rho_r^2 gR_0^3}{\mu_r^2}\quad Mc=\left(\frac{\rho_r U_{00}^2}{P_0}\right)^{1/2}$$
$$\bar{Re}=\frac{\bar{\rho}_r U_{00}R_0}{\bar{\mu}_r}\quad \bar{Pr}=\frac{\bar{\mu}_r\bar{c}_{pr}}{\bar{k}_r}\quad \bar{Sc}=\frac{\bar{\mu}_r}{\bar{\rho}_r\bar{D}_r}$$
$$\bar{Gr}=\frac{\bar{\rho}_r^2 gR_0^3}{\bar{\mu}_r^2}\quad \bar{Mc}=\left(\frac{\bar{\rho}_r U_{00}^2}{P_0}\right)^{1/2} \tag{6}$$

where g is the acceleration of gravity.

At the flow inlet, $x=0$ for co-current flows or $x=L$ for counter-current flows, the vapor mixture has a fully developed velocity profile with a saturation state corresponding to the inlet temperature T_{00} and the inlet pressure P_0;

$$u=1-r^2\quad \theta=1\quad C=C_{00}(T_{00},P_0). \tag{7}$$

The channel wall is cooled isothermally at a constant temperature T_w between $x=0$ and $x=L$; $\theta=0$. Film condensation starts at $x=0$ with zero film thickness and has a thickness $\delta(x)$ at the point x;

$$\delta(0)=0. \tag{8}$$

This implies that the wall surface preceding the cooled one should be kept at the same temperature as that of the vapor mixture. Since no transition layer from the vapor phase to the liquid phase is assumed, the liquid–vapor interface is located radially at

$$R_\delta=R-\delta. \tag{9}$$

At the interface, the no-slip condition of axial velocity and temperature gives

$$\bar{u}_i=u_i \tag{10}$$

$$\bar{\theta}_i=\theta_i. \tag{11}$$

The continuity of fluxes of mass, momentum, species and energy across the interface can be expressed as

$$\frac{\bar{\rho}_r}{\rho_r}\left[\bar{\rho}\left(\bar{v}-\bar{u}\frac{\mathrm{d}R_\delta}{\mathrm{d}x}\right)\right]_i=\left[\rho\left(v-u\frac{\mathrm{d}R_\delta}{\mathrm{d}x}\right)\right]_i\equiv\dot{m} \tag{12}$$

$$\frac{\bar{\mu}_r}{\mu_r}\left(\bar{\mu}\frac{\partial\bar{u}}{\partial r}\right)_i=\left(\mu\frac{\partial u}{\partial r}\right)_i \tag{13}$$

$$\left[\dot{m}\bar{C}-\frac{\bar{\rho}_r}{\rho_r ReSc}\left(\bar{\rho}\bar{D}\frac{\partial\bar{C}}{\partial r}\right)\right]_i = \left[\dot{m}C-\frac{1}{ReSc}\left(\rho D\frac{\partial C}{\partial r}\right)\right]_i \tag{14}$$

$$\left(-\bar{k}\frac{\partial\bar{\theta}}{\partial r}\right)_i-\frac{k_r}{\bar{k}_r}\left(-k\frac{\partial\theta}{\partial r}\right)_i = \frac{\rho_r}{\bar{\rho}_r}\frac{\bar{Re}\bar{Pr}}{He}\dot{m}\lambda-\frac{\bar{Pr}}{He\bar{Sc}}\left[(\lambda_1-\lambda_2)\bar{\rho}\bar{D}\frac{\partial\bar{C}}{\partial r}\right]_i \tag{15}$$

where the assumption of slow change of the channel radius and the film thickness in the axial direction is employed and λ denotes the latent heat of vaporization of the mixture referred to the liquid state. The mass condensation rate per unit area of the interface $\dot{m}$ is nondimensionalized by $\rho_r U_{00}$. The non-dimensionalized parameter He is defined as

$$He=\frac{\bar{c}_{pr}(T_{00}-T_w)}{\lambda_r}.$$

Further, the condition of thermodynamic equilibrium at the interface specifies definite interfacial mass fractions of the component vapor and the component liquid corresponding to the interfacial temperature T_i and the pressure p;

$$\bar{C}_i=\bar{C}_e(T_i,p)\quad C_i=C_e(T_i,p). \tag{16}$$

The set of these governing equations subject to the boundary conditions may afford the solution of binary mixture film condensation in a vertical channel by

means of finite difference methods. However, a significant difficulty remains in the inevitable requirement of extensive computation for such numerical solutions. Fortunately, for practical values of liquid flow properties, it has been found that the convective terms in the conservation equations play an insignificant role. Hence, the so-called Nusselt solution can be employed for the liquid film flow. From the practical point of view, not detailed informations about the distribution of vapor flow variables but the integrated values at the flow boundaries are likely to be much discussed. For this purpose, solutions of the system can be examined with the integral method by assuming appropriate profile for the distribution of flow variables.

By neglecting the convective terms and assuming thin film thickness compared with the channel radius, equations (1)–(4) for the liquid flow lead to the following solutions,

$$\bar{u} = \frac{\delta^2}{2\bar{\mu}}\left(\frac{\bar{R}e}{\bar{M}c^2}\frac{\mathrm{d}p}{\mathrm{d}x} - \frac{\bar{G}r}{\bar{R}e}\bar{\rho}\right) \times \left[\left(\frac{R-r}{\delta}\right)^2 - \frac{R-r}{\delta}\right] + u_i\frac{R-r}{\delta} \tag{17}$$

$$\bar{C} = \bar{C}_i \tag{18}$$

$$\bar{\theta} = \theta_i\frac{R-r}{\delta} \tag{19}$$

where the wall surface is assumed to be impermeable to both components of the mixture and to allow no-slip flow.

Integration of equations (1)–(4) for the vapor mixture with respect to r from the center to the interface yields

$$\frac{\mathrm{d}}{\mathrm{d}x^*}\int_0^{R_\delta}\rho u r\,\mathrm{d}r + \dot{m}^* R_\delta = 0 \tag{20}$$

$$\frac{\mathrm{d}}{\mathrm{d}x^*}\int_0^{R_\delta}\rho u u r\,\mathrm{d}r + \dot{m}^* u_i R_\delta = \int_0^{R_\delta}\left(-\frac{1}{Mc^2}\frac{\mathrm{d}p}{\mathrm{d}x^*} + \frac{GrSc}{Re}\rho\right)r\,\mathrm{d}r + ScR_\delta\left(\mu\frac{\partial u}{\partial r}\right)_i \tag{21}$$

$$\frac{\mathrm{d}}{\mathrm{d}x^*}\int_0^{R_\delta}\rho u C r\,\mathrm{d}r + \dot{m}^* C_i R_\delta = R_\delta\left(\rho D\frac{\partial C}{\partial r}\right)_i \tag{22}$$

$$\frac{\mathrm{d}}{\mathrm{d}x^*}\int_0^{R_\delta}\rho u c_p\theta r\,\mathrm{d}r + \dot{m}^* c_p\theta_i R_\delta = \frac{Sc}{Pr}R_\delta\left(k\frac{\partial\theta}{\partial r}\right)_i + \int_0^{R_\delta}\rho c_p' D\frac{\partial C}{\partial r}\frac{\partial\theta}{\partial r}r\,\mathrm{d}r \tag{23}$$

where, from the viewpoint of similarity, the following nondimensional variables are introduced by the inspection into the governing equations and boundary conditions.

$$x = ReScx^* \quad ReSc\dot{m} = \dot{m}^* \quad ReScv = v^*. \tag{24}$$

With equations (17)–(19), the boundary conditions, equations (12)–(15), are reduced to

$$\frac{\bar{\rho}_r}{\rho_r}\left[\rho\left(v^* - u\frac{\mathrm{d}R_\delta}{\mathrm{d}x^*}\right)\right]_i = \left[\rho\left(v^* - u\frac{\mathrm{d}R_\delta}{\mathrm{d}x^*}\right)\right]_i = \dot{m}^* \tag{25}$$

$$\frac{\delta}{2}\left(\frac{\bar{R}e}{\bar{M}c^2ReSc}\frac{\mathrm{d}p}{\mathrm{d}x^*} - \frac{\bar{G}r}{\bar{R}e}\bar{\rho}\right) - \bar{\mu}\frac{u_i}{\delta} = -\frac{\mu_r}{\bar{\mu}_r}\left(\mu\frac{\partial u}{\partial r}\right)_i \tag{26}$$

$$\dot{m}^*\bar{C}_i = \dot{m}^* C_i - \left(\rho D\frac{\partial C}{\partial r}\right)_i \tag{27}$$

$$\bar{k}\frac{\theta_i}{\delta} + \frac{k_r}{\bar{k}_r}\left(k\frac{\partial\theta}{\partial r}\right)_i = \frac{\rho_r\bar{R}e\bar{P}r}{\bar{\rho}_r HeReSc}\dot{m}^*\lambda. \tag{28}$$

As the vapor mixture proceeds along the cooled wall, the effect of condensation penetrates into its center of flow and a layer of boundary-layer type concerning the mass fraction and temperature is formed. By assuming a parabolic profile, the radial distribution of mass fraction and temperature can be expressed as

$$C = \begin{cases} C_0\,. & 0 \leqslant r < R_c \\ C_0 + (C_i - C_0)\left(\dfrac{r-R_c}{R_\delta - R_c}\right)^2 & R_c \leqslant r \leqslant R_\delta \end{cases} \tag{29}$$

$$\theta = \begin{cases} \theta_0 & 0 \leqslant r < R_t \\ \theta_0 + (\theta_i - \theta_0)\left(\dfrac{r-R_t}{R_\delta - R_t}\right)^2 & R_t \leqslant r \leqslant R_\delta. \end{cases} \tag{30}$$

R_c and R_t may be called as the radius of the concentration and temperature layers, respectively. The mass fraction and temperature at the center, C_0 and θ_0, are kept constant before the layer reaches the center, say, in the developing region; $C_0 = C_{00}(R_c > 0)$, $\theta_0 = 1(R_t > 0)$. Beyond the distance at which the layer has extended throughout the cross-section of the flow passage, say, in the developed region, they are forced to change axially;

$C_0 = C_0(x)(R_c = 0)$, $\theta_0 = \theta_0(x)(R_c = 0)$. The axial velocity profile is assumed to be

$$u = u_0 + (u_i - u_0)\left(\frac{r}{R_\delta}\right)^2 \tag{31}$$

where at the flow inlet, $x = 0$ (co-current flow) or $x = L$ (counter-current flows), $u_0 = 1$ and $u_i = 0$.

With these radial distributions of velocity, mass fraction and temperature, the integrals in equations (20)–(23) can be expressed in terms of the values at the center and the interface, if the involved physical properties are evaluated at an appropriate reference state so as to be regarded as constant across the layer. Then, equations (20)–(23) are reduced to ordinary differential equations as follows.

$$\frac{\mathrm{d}}{\mathrm{d}x^*}\left\{R_\delta^2\left[\frac{\rho_r}{4\bar{\rho}_r}\rho(u_0+u_i)+\tfrac{1}{3}\bar{\rho}\frac{\delta}{R_\delta}\left(2u_i-\frac{\mu_r}{\bar{\mu}_r}\frac{\mu}{\bar{\mu}}\frac{u_0-u_i}{R_\delta}\delta\right)\right]\right\}=0 \tag{32}$$

$$\left(1+\frac{\delta}{R_\delta}\right)\frac{R_\delta^2}{2Mc^2}\frac{\mathrm{d}p}{\mathrm{d}x^*}=\frac{\bar{G}r}{2}\frac{ReSc}{\bar{R}e^2}R_\delta^2\left(\rho+\frac{\bar{\rho}_r\bar{\rho}}{\rho_r}\frac{\delta}{R_\delta}\right)$$
$$-\frac{\mathrm{d}}{\mathrm{d}x^*}\left[\frac{\rho}{6}R_\delta^2(u_0^2+u_0u_i+u_i^2)\right]-u_i\left[\dot{m}^*R_\delta+Sc\frac{\bar{\mu}_r\bar{\mu}}{\mu_r}\frac{R_\delta}{\delta}\right] \tag{33}$$

$$\frac{\mathrm{d}}{\mathrm{d}x^*}\left\{\frac{\rho(C_i-C_0)}{12}\left[\frac{u_0-u_i}{5R_\delta^2}(R_c-R_\delta)^2(R_c^2+4R_cR_\delta+5R_\delta^2)-u_i(R_c^2+2R_cR_\delta-3R_\delta^2)\right]\right\}$$
$$=(C_i-C_0)R_\delta\left\{\frac{2\rho D}{R_\delta-R_c}-\dot{m}^*\right\} \tag{34}$$

$$\frac{\mathrm{d}}{\mathrm{d}x^*}\left\{\frac{\rho c_p(\theta_i-\theta_0)}{12}\left[\frac{u_0-u_i}{5R_\delta^2}(R_t-R_\delta)^2(R_t^2+4R_tR_\delta+5R_\delta^2)-u_i(R_t^2+2R_tR_\delta-3R_\delta^2)\right]\right\}$$
$$=(\theta_i-\theta_0)R_\delta\left\{\frac{Sc}{Pr}\frac{2k}{R_\delta-R_t}-c_p\dot{m}^*\right\}+\rho c_p'D(\theta_i-\theta_0)(C_i-C_0)S_{tc} \tag{35}$$

where

$$S_{tc}=4\left(\frac{R_\delta-R_t}{R_\delta-R_c}\right)^2\left[\frac{R_t-R_c}{R_\delta-R_t}\left(\frac{R_t}{R_\delta-R_t}\frac{1-\sigma^2}{2}+\frac{1-\sigma^3}{3}\right)+\left(\frac{R_t}{R_\delta-R_t}\frac{1-\sigma^3}{3}+\frac{1-\sigma^4}{4}\right)\right]$$

where

$$\sigma=0(R_c\leqslant R_t),\quad \frac{R_c-R_t}{R_\delta-R_t}(R_c>R_t).$$

From these equations, the axial change of u_0, p, R_c and R_t can be obtained. In the developed region ($R_c = 0$, $R_t = 0$), the last two equations are replaced by, respectively,

$$\frac{\mathrm{d}}{\mathrm{d}x^*}\left\{\frac{\rho}{12}R_\delta^2[(2u_0+u_i)C_0+(u_0+2u_i)C_i]\right\}=-\dot{m}^*\bar{C}_iR_\delta \tag{36}$$

$$\frac{\mathrm{d}}{\mathrm{d}x^*}\left\{\frac{\rho c_p}{12}R_\delta^2[(2u_0+u_i)\theta_0+(u_0+2u_i)\theta_i]\right\}=R_\delta\left\{\frac{2kSc}{Pr}\frac{\theta_i-\theta_0}{R_\delta}-\dot{m}^*c_p\theta_i\right\}+\rho c_p'D(C_i-C_0)(\theta_i-\theta_0) \tag{37}$$

from which C_0 and θ_0 are calculated.

The continuity condition of shearing stress at the interface, equation (26), gives the interfacial velocity u_i,

$$u_i\left(1+2\frac{\mu_r}{\bar{\mu}_r}\frac{\mu}{\bar{\mu}}\frac{\delta}{R_\delta}\right)=\frac{\delta^2}{2\bar{\mu}}\left(\frac{\bar{G}r}{\bar{R}e}\bar{\rho}-\frac{\bar{R}e}{\bar{M}c^2ReSc}\frac{\mathrm{d}p}{\mathrm{d}x^*}\right)+2\frac{\mu_r}{\bar{\mu}_r}\frac{\mu}{\bar{\mu}}\frac{\delta}{R_\delta}u_0. \tag{38}$$

By the continuity condition of energy flux at the interface, equation (28), the interfacial temperature θ_i is expressed as

$$\theta_i\left(1+2\frac{k_r}{\bar{k}_r}\frac{k}{\bar{k}}\frac{\delta}{R_\delta-R_t}\right)=2\frac{k_r}{\bar{k}_r}\frac{k}{\bar{k}}\frac{\delta}{R_\delta-R_t}\theta_0+\frac{\rho_r\bar{R}e\bar{P}r}{\bar{\rho}_rHeReSc}\frac{\lambda\delta}{\bar{k}}\dot{m}^*. \tag{39}$$

The mass flux of the condensate or the condensation rate per unit area of the interface $\dot{m}^*$ is given by the continuity of species mass flux, equation (27),

$$\dot{m}^*=\frac{2\rho D}{R_\delta-R_c}\frac{C_i-C_0}{C_i-\bar{C}_i}. \tag{40}$$

The continuity of mass, flux, equation (25), yields the film thickness,

$$\delta\frac{\mathrm{d}}{\mathrm{d}x^*}\left\{R\left|\frac{\bar\rho}{3\bar\mu}\left(Gr\bar\rho-\frac{\bar Re^2}{\bar Mc^2ReSc}\frac{\mathrm{d}p}{\mathrm{d}x^*}\right)\delta^3+\bar Re\bar\rho\frac{\mu_r}{\bar\mu_r}\frac{\mu}{\bar\mu}\frac{u_0}{R_o}\delta^2\right|\right\}$$

$$=\frac{HeReSc}{\bar Pr}\frac{R_o}{\lambda}\left\{\bar k\theta_i+\frac{2k_r}{\bar k_r}k(\theta_i-\theta_0)\frac{\delta}{R_o-R_c}\right\}. \tag{41}$$

When $u_0=0$, $\mathrm{d}p/\mathrm{d}x=0$ and $\theta_i=\theta_0$, it gives the Nusselt solution. The condensation rate of the volatile component $\dot m_c^*$ and the heat flux per unit wall surface q are then given by

$$\dot m_c^*=\dot m^*\bar C_i \tag{42}$$

$$q=\bar k\frac{\theta_i}{\delta} \tag{43}$$

where $\dot m_c$, $\dot m_c^*$ and q are nondimensionalized by ρ_rU_{00}, ρ_rD_r/R_0 and $\bar k_r(T_{00}-T_w)/R_0$, respectively.

The set of these ordinary differential equations can be solved numerically by means of finite difference method stepwise in the flow direction. Since the equations contain thermophysical properties of vapor and liquid mixtures, knowledge of them is required to such a numerical study.

For the binary mixtures under consideration in the present study, the phase equilibrium condition, that is, equality of the chemical potentials of each component in liquid and vapor phases, can be well approximated as

$$X_jp=\bar\gamma_j\bar X_jp_{sj}\quad(j=1,2) \tag{44}$$

where X_j is the mole fraction, $\bar\gamma_j$ the activity coefficient of species j in the liquid phase and p_{sj} the vapor pressure of pure component j. The activity coefficients are evaluated by the Van Laar equation with empirical constants given by Hála *et al.* [12]

$$\log\bar\gamma_1=\frac{A_{12}}{\left(1+\frac{A_{12}\bar X_1}{A_{21}\bar X_2}\right)^2}\qquad\log\bar\gamma_2=\frac{A_{21}}{\left(1+\frac{A_{21}\bar X_2}{A_{12}\bar X_1}\right)^2}. \tag{45}$$

The vapor pressure of pure component j is predicted by the Antoine equation

$$\log p_{sj}=A_j-\frac{B_j}{T+C_j}\quad(j=1,2) \tag{46}$$

where constants A_j, B_j and C_j are also given in [12]. The equilibrium mole fractions of the component liquids and vapors are then given by

$$\bar X_1=\frac{p-\bar\gamma_2p_{s2}}{\bar\gamma_1p_{s1}-\bar\gamma_2p_{s2}}\qquad X_1=\frac{1}{1+\frac{\bar\gamma_2}{\bar\gamma_1}\frac{p_{s2}}{p_{s1}}\frac{\bar X_2}{\bar X_1}}. \tag{47}$$

For the transport properties of viscosity, thermal conductivity and binary diffusion coefficients are estimated by the way recommended by Bretsznajder [13]. Densities and specific heats of pure component are evaluated by algebraic equations of the second order of temperature with the data in [14]. The latent heat of vaporization of pure component is calculated by the Clasius–Clapeyron relation with equation (46).

At an appropriate reference state, the physical properties involved in the governing equations are evaluated to be regarded as constant across the flows. As for such a reference state, although a definitive recommendation is not available, the arithmetical mean state of the center and the interface is chosen for the vapor mixture flow; that is, the properties are evaluated at

$$T_r=(T_0+T_i)/2\quad C_r=(C_0+C_i)/2.$$

For the liquid-phase properties, on the basis of [2], the reference state is taken as

$$\bar T_r=T_w+(T_i-T_w)/3\quad\bar C_r=\bar C_i.$$

As for the reference values of physical properties for nondimensional parameters, it is convenient to evaluate them at the flow inlet state for the vapor, $T_r=T_{00}$, $C_r=C_e(T_{00})=C_{00}$, and at the state of the wall for the liquid, $\bar T_r=T_w$, $\bar C_r=\bar C_i(T_w)$.

3. RESULTS AND DISCUSSIONS

By employing the foregoing physical model and analytical method, film condensation of binary mixtures in a vertical channel is studied for vapor mixtures of ethanol–water, methanol–water, acetone–water, methanol–ethanol and hexane–benzene. Effects of the channel geometry, the inlet-flow velocity and temperature, the vapor flow direction and the wall temperature are investigated. Three different types of circular channel are used as for the variation of channel geometry, having divergent, constant and convergent cross-sections with respect to the flow direction:

$R(x)=1+0.1x$ diffuser-type flow (D);
$R(x)=1$ constant cross-section flow (C);
$R(x)=1-0.05x$ nozzle-type flow (N);

of which the ratio of peripherical areas is 2:1:1/2 and the ratio of cross-sections 4:1:1/4 at $x=10$.

The equations are solved stepwise in the gas flow direction by means of finite difference method. To deal with the singularity at the inlet of co-current flow, an analytical solution obtained by expanding the variables with respect to x is employed close to the inlet. For counter-current flows, the vapor mixture has a zero-velocity point close to the interface. Between this zero-velocity point and the channel center, the vapor mixture at the flow inlet is assumed to have a uniform temperature (mass fraction), and in the annular region between the zero-velocity point and the wall the vapor is sucked in together with the liquid in the same direction. In this case, iterative computation is required to achieve compatibility with the liquid film of zero thickness at $x=0$.

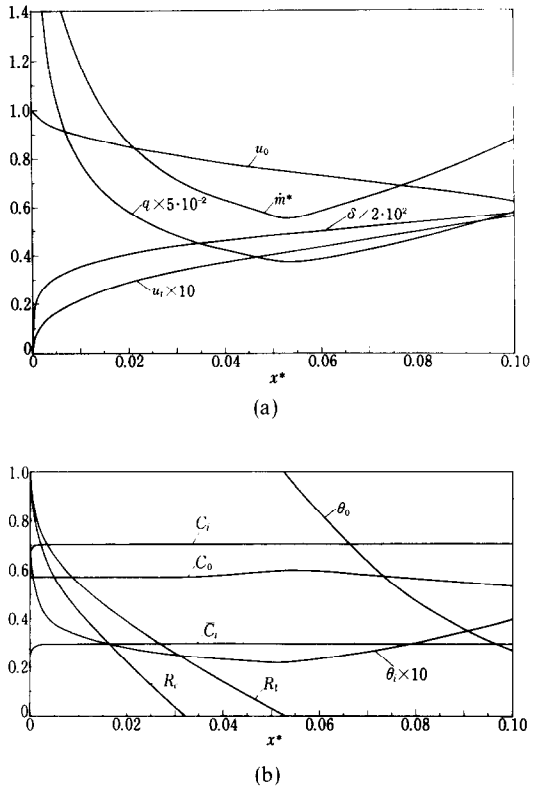

FIG. 2. Co-current flow film condensation; ethanol–water, constant cross-section, $T_{00} = 90°C$, $T_w = 85°C$, $U_{00} = 10\,cm/s$. (a) $\dot{m}^*$, q, δ, u_0, u_i. (b) R_c, R_t, θ_0, θ_i, C_0, C_i, $\bar{C}_i$.

A typical result of film condensation behavior is shown in Fig. 2 for the case of ethanol–water mixture in a constant cross-section channel ($R_0 = 1\,cm$) with $T_{00} = 90°C$ ($C_{00} = 0.507$), $T_w = 85°C$ and $U_{00} = 10\,cm/s$; $Re = 101$, $\bar{R}e = 1511$, $Pr = 0.926$, $\bar{P}r = 5.03$, $Sc = 0.636$, $Gr = 1.00\times10^5$, $\bar{G}r = 2.24\times10^7$, $Mc = 0.341\times10^{-3}$, $\bar{M}c = 0.971\times10^{-2}$. The condensation rate per unit interface area decreases first rapidly in the flow direction and reaches a minimum at the point close to the end of the developing region. After taking the minimum, it increases again, although the behavior of this increase is dominated considerably by the temperature difference of the system and the type of binary mixture (cf. Figs. 5 and 6). The first decrease of the rate is contributed to the growth of concentration layer which reduces the diffusion flux of the volatile component from the interface to the bulk flow. The increase of the rate after the minimum can be attributed mainly from the axial decrease in the mass fraction of the volatile component in the bulk. After the end of the developing region, the mass fraction of the volatile component in the main stream increases due to higher diffusion fluxes from the interface to the bulk than the convective flux which is always oriented toward the interface. Further condensation, however, leads to the superiority of the convective flux to the diffusion flux which decreases the mass fraction in the bulk. Under some conditions, this increase in the condensation rate accelerates the tendency of decreasing mass fraction in the bulk to result in a very rapid increase in the condensation rate in the developed region. The heat flux to the wall has the same behavior as the condensation rate since it is approximately proportional to the latter. Because of small difference of the interfacial temperature from the wall temperature, the mass fractions at the interface hardly have an appreciable variation in the axial direction. The concentration and temperature layers develop as $(R_0 - R_{c,t}) \propto x^{0.4}$. The condensation rate and the film thickness in the developing region change roughly as $\dot{m} \propto x^{-0.4}$ and $\delta \propto x^{0.2}$, respectively. The interfacial temperature is dominated mainly by the film thickness and the condensation rate, being approximately proportional to them. The interfacial velocity shows a similar behavior as the film thickness, being approximately proportional to the square of the latter. It should be noted that the rapid reduction in the main stream temperature of vapor mixture in the developed region could result in a super-saturation state of the vapor, that is, a possibility of dropwise condensation in the vapor flow which is not accounted for in the present study.

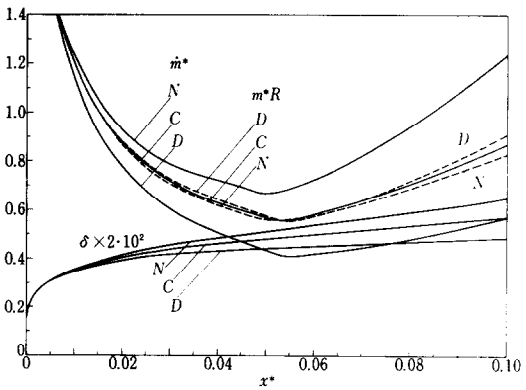

FIG. 3. Effect of channel geometry (N: nozzle, C: constant, D: diffuser); ethanol–water, $T_{00} = 90°C$, $T_w = 85°C$, $U_{00} = 10\,cm/s$.

In Fig. 3, the effect of the channel geometry is presented for co-current flows. The condensation rate per unit interface area is greatly reduced for the diffuser-type flow, whereas onto the wall of the nozzle-type channel the mixture condenses at considerably higher rates. Upon the overall condensate mass or the condensation mass flux per unit axial length, $\dot{m}^*R$, however, the channel geometry has little influence; the diffuser flow yields rather slightly higher rates than the nozzle flow. It may be attributed to the compensation effect of axial variations between the condensation rate per unit interface area and the peripherical area of the interface. Owing to the axial change of cross-section area, the nozzle flow has larger values of the film thickness and the interfacial velocity and temperature than the diffuser flow has.

The effect of the vapor flow velocity is demonstrated in Fig. 4 in the expression of $\dot{m}ReSc$ vs $x/(ReSc)$. It means that the condensation rate nondimensionalized by $\rho_v D_v/R_0$ should be characterized by the Reynolds number based on the axial length and the inlet velocity

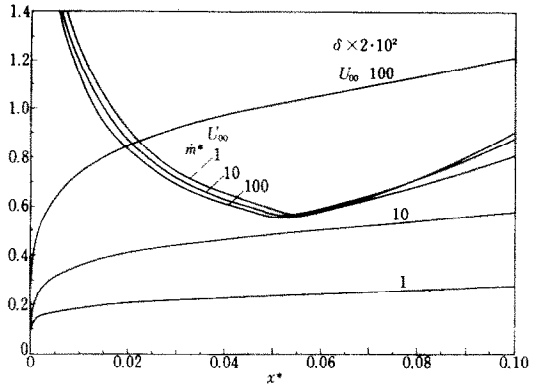

FIG. 4. Effect of vapor flow velocity (U_{00} cm/s); ethanol–water, constant cross-section, $T_{00} = 90°C$, $T_w = 85°C$.

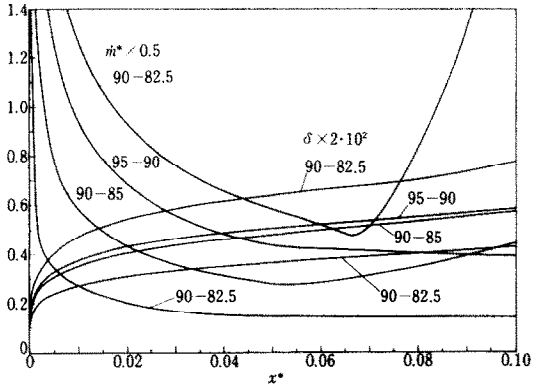

FIG. 5. Effect of flow and wall temperatures ($T_{00} - T_w$ °C); ethanol–water, constant cross-section, $U_{00} = 10$ cm/s.

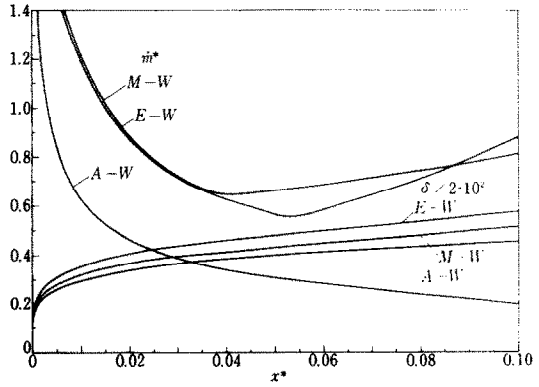

FIG. 6. Effect of type of binary mixture (E–W: ethanol–water, M–W: methanol–water, A–W: acetone–water); constant cross-section, $T_{00} = 90°C$, $T_w = 85°C$, $U_{00} = 10$ cm/s.

of the vapor mixture. Higher flow velocities result in lower condensation rates and shorter lengths of developing regions of concentration and temperature at the same axial Reynolds number.

The vapor temperatures at the inlet and the wall temperature have a considerable effect on the behavior of film condensation. As shown in Fig. 5, larger differences between them result in higher condensation rates. The type of binary mixture also has an appreciable effect through its equilibrium characteristics, as shown in Fig. 6. These behaviors can be characterized by the factor of mass fraction differences

$$[C_{00} - C_e(T_w)]/[\bar{C}_e(T_\infty) - C_e(T_w)],$$

which means the ratio of the driving force of diffusion process to the potential barrier of condensation of the volatile component; 0.337 (E–W), 0.340 (M–W), 0.117 (A–W). Larger values of this factor yield higher condensation rates. It is seen from this fact that when the vapor inlet temperature and the wall temperature are changed simultaneously with keeping a constant difference, the condensation rate will take a minimum at the temperature close to which the difference of mass fractions, $C_e(T) - \bar{C}_e(T)$, becomes maximum. Higher condensation rates are always associated with higher interfacial temperatures and longer lengths of developing layers of concentration and temperature. The film thickness is approximately proportional to the one-third power of the factor and varies as $\delta \propto x^n$ with $n = 0.15 \sim 0.25$. The pressure gradient is roughly proportional to $\delta \bar{G}r/Re\bar{R}e$ or $(\bar{G}r/\bar{R}e)^{2/3}/Re$.

A typical result of film condensation of counter-current flows is shown in Fig. 7 for ethanol–water mixture with the same condition as in Fig. 2: $T_{00} = 90°C$, $T_w = 85°C$, $U_{00} = -10$ cm/s, and $L/R_0 = 10$ ($R_0 = 1$ cm). The concentration and temperature layers of the vapor mixture develop from the outlet of the condensate film flow. Because of relatively small variation of condensation rate at the beginning of the film flow (in the developed region), the film thickness is

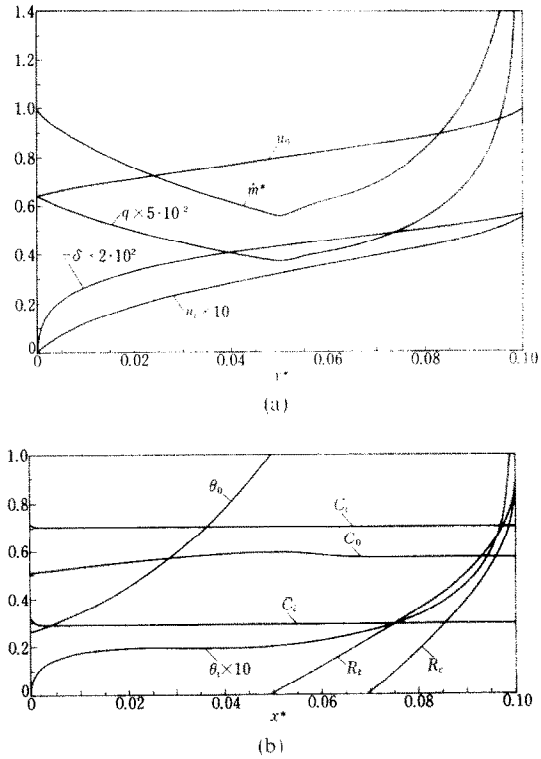

FIG. 7. Counter-current flow film condensation; ethanol–water, constant cross-section, $T_{00} = 90°C$, $T_w = 85°C$, $U_{00} = -10$ cm/s. (a) $\dot{m}^*$, q, δ, u_0, u_i. (b) R_c, R_i, θ_0, θ_i, C_0, C_i, $\bar{C}_i$.

thinner and varies more rapidly in the x-direction as $\delta \propto x^n$ with $n = 0.25 \sim 0.3$ than that for the co-current flow. Further, in the developing region of concentration, it changes more sharply ($n > 0.3$). Due to this fact, the interfacial velocity also changes more sharply in the x-direction compared with that of the co-current flow. The interfacial temperature, thus, the mass fraction at the interface shows somewhat different behaviors close to the beginning of the liquid film flow, approaching the wall temperature at $x = 0$.

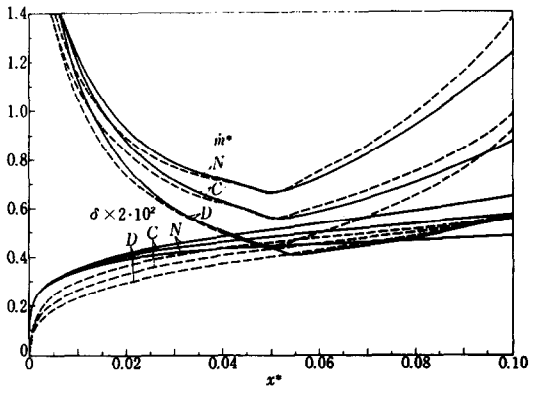

FIG. 8. Effect of flow direction (—: co-current flow, – –: counter-current flow); ethanol–water, $T_{00} = 90°C$, $T_w = 85°C$, $|U_{00}| = 10\,cm/s$.

The effect of the channel geometry of counter-current flows is shown in Fig. 8 in comparison with that of co-current flows. The geometry is termed with respect to the vapor flow. From the standpoint of liquid film flow, the "nozzle" in counter-current flows corresponds to the "diffuser" in co-current flows. As the case of co-current flows, the nozzle flow yields larger values of the condensation rate per unit interface area, the heat flux to the wall, the film thickness, and the interfacial velocity and temperature. Concerning the overall condensation rate and heat flux, the diffuser flow takes slightly larger values than the nozzle flow. This implies that the flow behavior might not be so appreciably affected by the flow direction as to yield fundamental change in the mass transport process of vapor components for film condensation.

4. CONCLUSION

Film condensation of binary-mixture laminar flows in a vertical channel of variable cross-section is studied by using the integral method for the vapor flow and the Nusselt model for the condensate flow. The two flow fields coupled with the interfacial conditions are solved numerically to predict the effects of the channel geometry, the vapor flow speed and direction, the inlet and wall temperatures and the type of binary mixtures on the behavior of film condensation. At the boundary between the vapor and the condensate, an infinitesimally thin layer of mixtures is assumed to be in liquid–vapor equilibrium. A saturated vapor mixture is introduced downward or upward into a vertical channel of variable circular cross-section. At the inlet, the vapor mixture has a fully developed profile of velocity and a uniform temperature. The channel wall is cooled isothermally at a constant temperature.

The film condensation is affected appreciably by the liquid–vapor equilibrium characteristics and the mass transfer process in the vapor mixture. The condensation rate decreases rapidly in the developing region due to the growth of concentration layer. After taking a minimum, it tends to increase again in the developed region owing to the behavior of mass transfer. The magnitude of condensation rate is characterized by the ratio of the difference of mass fractions at the inlet and the wall state to that of equilibrium mass fractions of the vapor and the liquid at the wall state. The heat flux to the wall has the same features as the condensation rate. The film thickness varies in the direction of gravity with the exponent power of 0.15–0.3 depending on the channel geometry, the flow direction, the temperature difference and the type of mixture. The interfacial temperature also shows very different behaviors depending on these flow conditions, although there is found small difference of temperatures at the interface and the wall. The interfacial mass fractions hardly change in the flow direction.

The nozzle-type flow always yields larger values of the condensation rate, heat flux, film thickness, and interfacial velocity and temperature compared with those of the diffuser-type flow. Due to the compensat-effect of axial changes in the condensation rate and the peripherical surface area, the overall condensation rate is not affected considerably by the channel geometry. The developing process of concentration and temperature layers of the vapor mixture is not appreciably influenced by the flow direction. After developed, especially close to the flow outlet, the flow direction has a considerable effect on condensation. The effect of vapor-flow velocity on the condensation rate can be expressed nondimensionally by the Reynolds number based on the distance from the flow inlet.

Acknowledgement—The author wishes to thank Prof. K. Oswatitsch for many stimulating and informative discussions throughout the course of the study.

REFERENCES

1. A. P. Colburn and T. B. Drew, The condensation of mixed vapors, *Trans. Am. Inst. Chem. Engrs* **33**, 157 (1937).
2. E. M. Sparrow and E. Marschall, Binary, gravity-flow film condensation, *J. Heat Transfer* **91C**, 205–211 (1969).
3. V. E. Denny and V. J. Jusionis, Effects of forced flow and variable properties on binary film condensation, *Int. J. Heat Mass Transfer* **15**, 2143–2153 (1972).
4. V. E. Denny and V. South III, Effects of forced flow, noncondensables, and variable properties on film condensation of pure and binary vapors at the forward stagnation point of a horizontal cylinder, *Int. J. Heat Mass Transfer* **15**, 2133–2142 (1972).
5. A. Tamir, Condensation of binary mixtures of miscible vapors, *Int. J. Heat Mass Transfer* **16**, 683–685 (1973).
6. Y. Taitel and A. Tamir, Film condensation of multicomponent mixtures, *Int. J. Multiphase Flow* **1**, 697–714 (1974).
7. J. Bandrowski and A. Bryczkowski, Experimental study of heat transfer at the total condensation of mixed vapours of miscible liquids, *Int. J. Heat Mass Transfer* **18**, 503–512 (1975).

8. E. Marschall and J. A. Hall, Binary, gravity-flow film condensation, *J. Heat Transfer* **97**, 492–494 (1975).
9. J. P. Van Es and P. M. Heertjes, The condensation of a vapor of a binary mixture, *Br. Chem. Engng* **8**, 580–586 (1962).
10. E. Kirschbaum and E. Tröster, Untersuchungen zum Stoffübergang bei der Teilkondensation von Gemischdampfen, *Chemie-Ingr-Tech.* **32**, 395 (1960).
11. E. Tröster, Berechnung der Trennwirkung von Teilkondensation (Dephlegmatoren), *Chemie-Ingr-Tech.* **32**, 525–531 (1960).
12. E. Hála, I. Wichterle, J. Polák and T. Boublík, *Vapour–Liquid Equilibrium Data at Normal Pressures*. Pergamon Press, Oxford (1968).
13. S. Bretsznajder, *Prediction of Transport and Other Physical Properties of Fluids*. Pergamon Press, Oxford (1971).
14. *VDI Wärmeatlas*. Deutscher Ingenieur, Dusseldorf (1953).

CONDENSATION EN FILM D'UN ECOULEMENT BINAIRE DANS UN CANAL VERTICAL

Résumé—On étudie la condensation en film d'écoulements binaires dans un canal vertical à section circulaire variable, en employant la méthode intégrale pour un écoulement de vapeur et le modèle de Nusselt pour le film liquide tombant. On détermine les effets de la géométrie du canal, de la vitesse de la vapeur, de la direction de l'écoulement de vapeur et du type de mélange binaire sur le comportement de la condensation. Ce comportement est sensiblement affecté par les caractéristiques de l'équilibre liquide-vapeur et le processus de transfert massique dans l'écoulement de vapeur. Les écoulements de type tuyère donnent de plus grandes valeurs du flux local de condensation bien que la géométrie du canal n'a pas un effet considérable sur le flux global de condensation. La direction de l'écoulement a une influence appréciable sur le flux de condensation et sur l'épaisseur de film.

FILMKONDENSATION BEI DER STRÖMUNG EINES BINÄREN GEMISCHES IN EINEM SENKRECHTEN KANAL

Zusammenfassung—Es wird die Filmkondensation bei laminarer Strömung eines binären Gemisches in einem senkrechten Kanal mit veränderlichem Querschnitt untersucht. Dabei wird für die Dampfströmung die Integralmethode und für die Flüssigkeitsfilmströmung das Nusselt-Modell angewandt. Die Einflüsse der Kanalgeometrie, der Dampfströmungsgeschwindigkeit, der Dampfströmungsrichtung und der Art des binären Gemisches auf das Kondensationsverhalten werden vorhergesagt. Das Verhalten wird deutlich durch die Flüssigkeit/Dampf-Gleichgewichtseigenschaften und den Stofftransportvorgang in der Dampfströmung beeinflußt. Düsenströmungen erreichen höhere Werte für die örtliche Kondensationsrate, obwohl die Kanalgeometrie keinen erheblichen Einfluß auf die mittlere Kondensationsrate hat. Die Strömungsrichtung hat einen merklichen Einfluß auf die Kondensationsrate und die Filmdicke.

ПЛЕНОЧНАЯ КОНДЕНСАЦИЯ ПРИ ТЕЧЕНИИ БИНАРНОЙ СМЕСИ В ВЕРТИКАЛЬНОМ КАНАЛЕ

Аннотация — Пленочная конденсация при ламинарном течении бинарных смесей в вертикальном кольцевом канале переменного сечения исследуется с помощью интегрального метода для течения пара и модели Нуссельта для течения пленки жидкости. Определено влияние геометрии канала, скорости течения пара, направления потока пара и вида бинарной смеси на процесс конденсации. Особое влияние оказывают равновесные характеристики жидкости и пара и перенос массы в потоке пара. При истечении из сопла получаются более высокие значения скорости локальной конденсации, хотя геометрия канала не оказывает большого влияния на суммарную скорость конденсации. Направление потока значительно влияет на скорость конденсации и толщину пленки.